PRISMA Hyperspectral Satellite Imagery Application to Local Climate Zones Mapping

Alberto Vavassori[1], Daniele Oxoli[1], Giovanna Venuti[1], Maria Antonia Brovelli[1], Ali Badr Eldin Ali Mohamed[1], Afshin Moazzam[1], Mario Siciliani de Cumis[2], Patrizia Sacco[2], Deodato Tapete[3]

[1] Dept. of Civil and Environmental Engineering, Politecnico di Milano, Milano, Italy - (alberto.vavassori, daniele.oxoli, giovanna.venuti, maria.brovelli, alibadr, afshin.moazzam)@polimi.it
[2] Italian Space Agency (ASI), Matera, Italy - (mario.sicilianidecumis, patrizia.sacco)@asi.it
[3] Italian Space Agency (ASI), Roma, Italy - deodato.tapete@asi.it

Keywords: Local Climate Zones, Image Analysis, Spectral Separability, PRISMA Hyperspectral Satellite.

Abstract

The urban heat island effect exacerbates the vulnerability of cities to climate change, emphasizing the need for sustainable urban planning driven by data evidence. In the last decade, the Local Climate Zone (LCZ) model emerged as a key tool for categorizing urban landscapes, aiding in the development of urban temperature mitigation strategies. In this work, the contribution of hyperspectral satellite imagery to LCZ mapping, leveraging the Italian Space Agency (ASI)'s PRISMA satellite, is investigated. Mapping performances are compared with traditional multispectral-based LCZ mapping using Sentinel-2 satellite imagery. The Random Forest algorithm is utilized for LCZ classification, with evaluation conducted through spectral separability analysis and accuracy assessment between PRISMA and Sentinel-2 derived LCZ maps as well as with the benchmark LCZ Generator mapping tool. An initial experiment on the effect of PRISMA image pan-sharpening on LCZ spectral separability is also presented. Results obtained for Milan (Northern Italy) demonstrate the potential of hyperspectral imagery in enhancing LCZ identification compared to multispectral data, with promising improvements in LCZ maps overall accuracy. Finally, air temperature patterns within each LCZ class are explored, qualitatively confirming the influence of urban morphology on thermal comfort.

1. Introduction

The United Nations Sustainable Development Goal (SDG) 11 emphasizes ensuring the safety, resilience, and sustainability of cities and urban areas. With the ongoing escalation of climate change impacts, cities are increasingly vulnerable to various threats, among which the rising frequency, intensity, and duration of heat waves. This phenomenon, coupled with the rapid pace of urbanization, has led to the intensification of the Urban Heat Island (UHI) effect on a global scale. The UHI affects temperature patterns and heat fluxes within urban areas, posing significant challenges to public health, infrastructure, and overall urban livability (Kumar, 2021).

In the last decades, the scientific community has developed physical and conceptual models to measure the intensity of the UHI phenomenon, which is key for implementing evidence-based mitigation strategies. In this context, the Local Climate Zone (LCZ) model (Stewart and Oke, 2012) is a widely accepted classification system that categorizes urban landscapes into different types based on their morphological characteristics and land cover composition. These two factors mostly influence air temperature in urban areas. Characteristics patterns in temperature observations and findings of numerical modelling further support the categorization of urban environments into LCZs (Stewart et al., 2014, Lehnert et al., 2018).

LCZ maps are typically generated using established approaches, based on the use of Geographic Information System (GIS) and/or Remote Sensing (RS) datasets. Typical geodata sources include multispectral satellite imagery, land cover maps, topographic databases, and meteorological sensor observations. (Aslam and Rana, 2022). Recent studies have identified the potential of employing hyperspectral satellite imagery for LCZ mapping, offering increased accuracy compared to multispectral data owing to a more detailed characterization of the spectral properties of urban surfaces (Liang et al., 2023, Vavassori et al., 2023b).

Given the above, we present here a hybrid RS/GIS-based method for LCZ mapping leveraging multispectral Sentinel-2 and the innovative hyperspectral PRISMA (PRecursore IperSpettrale della Missione Applicativa) satellite data (Loizzo et al., 2019) along with ancillary urban canopy parameter layers for the description of the urban morphological characteristics such as buildings and trees heights. The selected testbed for this study is the Metropolitan City of Milan (Northern Italy).

To investigate the enhancement in LCZ identification and mapping when using PRISMA hyperspectral data as opposed to Sentinel-2 data, spectral separability analysis is carried out. The accuracy of the classified maps is assessed using quality metrics derived from confusion matrices as well as through comparisons with LCZ maps generated from the LCZ Generator benchmark method (Demuzere et al., 2021). An additional experiment on the effect of PRISMA image resolution enhancement through pan-sharpening on LCZ spectral separability is presented. Empirical results provide insight into the suitability of PRISMA images for improving LCZ mapping accuracies in comparison to traditional methods based on multispectral image classification.

Finally, air temperature distribution patterns within each LCZ class are explored through zonal statics computation to provide initial and explorative insight into the LCZ influence on urban thermal comfort in the study area.

The methodology described in this paper was developed within the "Local Climate Zone & Open Data Cube" (LCZ-ODC) project - funded by the Italian Space Agency (ASI) - primarily aimed to produce multitemporal LCZ maps and assess their correlation with urban thermal comfort, while eliciting and addressing user community needs through the parallel development of open-source software tools to facilitate the exploitation of the project outcomes. These last results were discussed in prior studies published by the authors (Oxoli et al., 2023, Vavassori et al., 2023a).

The remainder of the paper is as follows. Section 2 provides an overview of both data and analysis techniques employed in this study. Section 3 showcases and discusses a sample of the obtained results, while conclusions and future directions of this work are reported in Section 4.

2. Data and Methods

The proposed RS/GIS-based procedure for LCZ mapping relies on the supervised classification of PRISMA and Sentinel-2 imagery by using a Random Forest classifier. The classification is applied to a multitemporal stack of co-registered and temporally co-located PRISMA and Sentinel-2 acquisitions.

PRISMA images feature 30 m spatial resolution and 239 spectral bands ranging between Visible-NearInfraRed to Short-Wave InfraRed (400-2500 nm) (Loizzo et al., 2019). Each PRISMA scene also integrates a panchromatic band at 5 m spatial resolution. PRISMA Level-2D images were collected from the official mission portal (`https://prisma.asi.it`). Access to both archive and new tasking images was granted to the authors by ASI in the context of the LCZ-ODC project. Level-2A Sentinel-2 images (443-2190 nm, 13 spectral bands up to 10 m spatial resolution) were instead obtained from the Copernicus Open Access Hub, recently replaced by the new Copernicus Data Space Ecosystem (`https://dataspace.copernicus.eu`).

A total of six pairs of temporally co-located PRISMA and Sentinel-2 acquisitions were considered, covering the Metropolitan City of Milan area in the period February-August 2023. Training and testing samples were gathered to conduct classification and evaluate its quality. The samples were manually delineated based on RGB PRISMA image. Different sets of samples were collected for each PRISMA acquisition to accommodate seasonal changes in vegetated areas.

Before the classification, the band stacks for the two sensors were enriched with additional bands linking to urban morphological characteristics such as buildings and tree heights derived from regional geo-databases, and pre-processed to meet the format, extension and resolution of the satellite bands. Values of these additional bands were normalized in the [0-1] range to make them comparable with the reflectance data and therefore employable in the classification procedure (Vavassori et al., 2023a). Sample output LCZ maps are reported in Figure 1.

Accuracy assessment was performed to evaluate classification performances by deriving quality metrics from confusion matrices, using the testing samples, on both PRISMA and Sentinel-2 LCZ classified maps. The procedure was repeated for maps generated using the LCZ Generator tool (Demuzere et al., 2021) which represents a reference method for LCZ mapping (see Figure 2).

In parallel, a spectral separability analysis based on the Jeffries-Matusita distance (Richards and Jia, 2006) was performed to outline differences in class separability between Sentinel-2 and PRISMA data. This distance ranges between 0 and 2 and is computed pairwise for each LCZ class by exploiting the spectral signature of the original band stacks used in the classification. Distances close to 2 indicate perfect separability while distances tending to 0 indicate that signatures of classes are identical. Results from such analysis were used to evaluate the capability of PRISMA to outperform Sentinel-2 in LCZ class identification (see Figure 3).

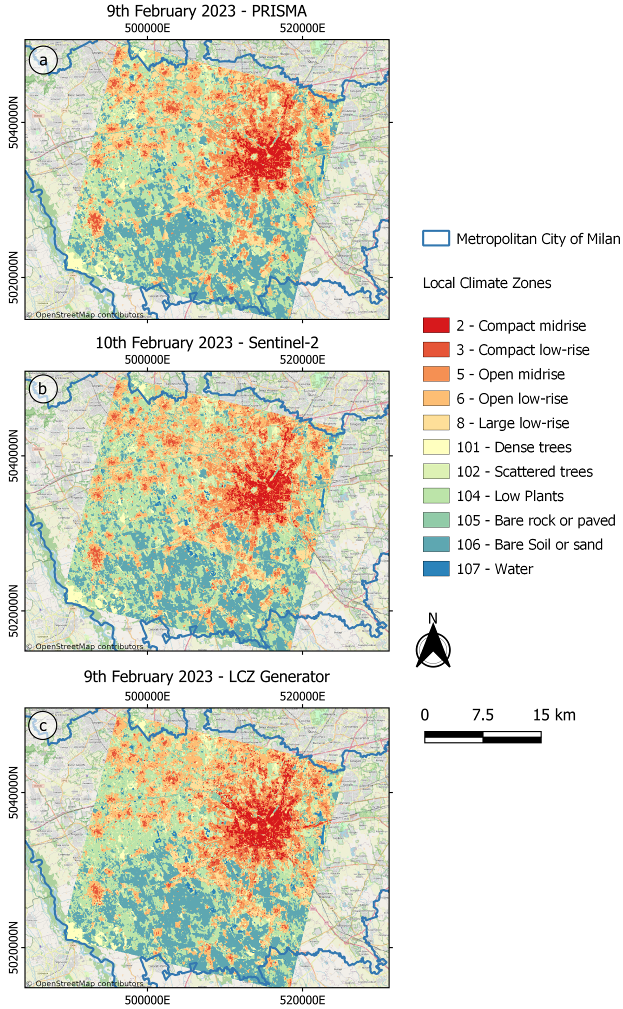

Figure 1. Sample LCZ maps obtained using (a) PRISMA, (b) Sentinel-2 and (c) the LCZ Generator for the Metropolitan City of Milan in February 2023. Coordinate Reference System: WGS84/UTM zone 32N - EPSG:32632.

A further experiment was conducted to examine the impact of hyperspectral pan-sharpening on the spectral separability of LCZ classes in PRISMA images. To that end, the Adaptive Gram-Schmidt decomposition method (Loncan et al., 2015) was applied to the Visible-NearInfraRed bands of PRISMA images (400-800 nm) using the panchromatic band at 5 m resolution. The spectral separability analysis was then iterated on both the pan-sharpened and the original PRISMA images, considering the Visible-NearInfraRed bands only (see Figure 4).

The classified LCZ maps were employed to conduct zonal statistics analysis on the distribution of air temperature. To that end, interpolated temperature maps from the ClimaMi project (`https://www.progettoclimami.it`) were used.

The ClimaMi project offers high-resolution spatial atlases of local climate variables for the Metropolitan City of Milan, encompassing seasonal average air temperature maps among other data sets. By overlaying these temperature maps with the LCZ maps, zonal statistics were computed and summarized in boxplots. These boxplots facilitated a qualitative examination of temperature patterns across different LCZ classes by providing insights into the interplay between urban morphology, land cover and temperature distributions (see Figure 5).

The methodologies employed in this work were implemented by developing a set of Python Jupyter notebooks. The complete codebase has been organized and made available on GitHub (`https://github.com/gisgeolab/LCZ-ODC`) to facilitate future reviews and replications of the case study discussed in this paper. The repository includes both the code and documentation divided into branches related to the scientific development tasks carried out in the context of the LCZ-ODC project.

3. Results

The accuracy assessment for the LCZ maps derived from both PRISMA and Sentinel-2 data indicated that PRISMA enhances LCZ detection, resulting in a mean Overall Accuracy (OA) increase of 7% for the six generated maps. Specifically, when examining confusion matrices derived from satellite acquisitions in February 2023, as illustrated in Figure 2, PRISMA consistently demonstrates better performance than Sentinel-2.

Furthermore, the comparison between the PRISMA and the LCZ Generator classified maps also produced promising results with a mean OA increase of 16%. A glimpse of these improvements is evident in the reduction of misclassifications as shown in Figure 2c).

The examination of spectral separability between individual LCZ class pairs reveals that the Jeffries-Matusita distances are notably greater for the spectral signatures derived from the PRISMA image compared to Sentinel-2. This observation suggests that leveraging hyperspectral data holds promise for enhancing the classification accuracy of LCZ maps.

The lower accuracy observed particularly in built-up LCZs can be attributed to heightened confusion between these classes, as depicted in Figure 2, aligning with their reduced spectral separability as illustrated in Figure 3. Additionally, within the land cover types, a slightly high level of confusion is discerned among some vegetated classes, namely Dense Trees, Scattered Trees, and Low Plants.

The application of pan-sharpening on the PRISMA image provided positive insights into the preservation of the LCZ spectral signature (see Figure 4a). In the same way, spectral separability after pan-sharpening showed similar performances in terms of Jeffries-Matusita distance values to the original PRISMA image (see Figure 4b).

The above suggests the suitability of the selected pan-sharpening algorithm to enhance the spatial resolution of LCZ maps without degrading the accuracy that would be obtained from the classification of the lower-resolution image. Spectral separability results differ from the previous test (see Figure 3) due to the use of a subset of bands.

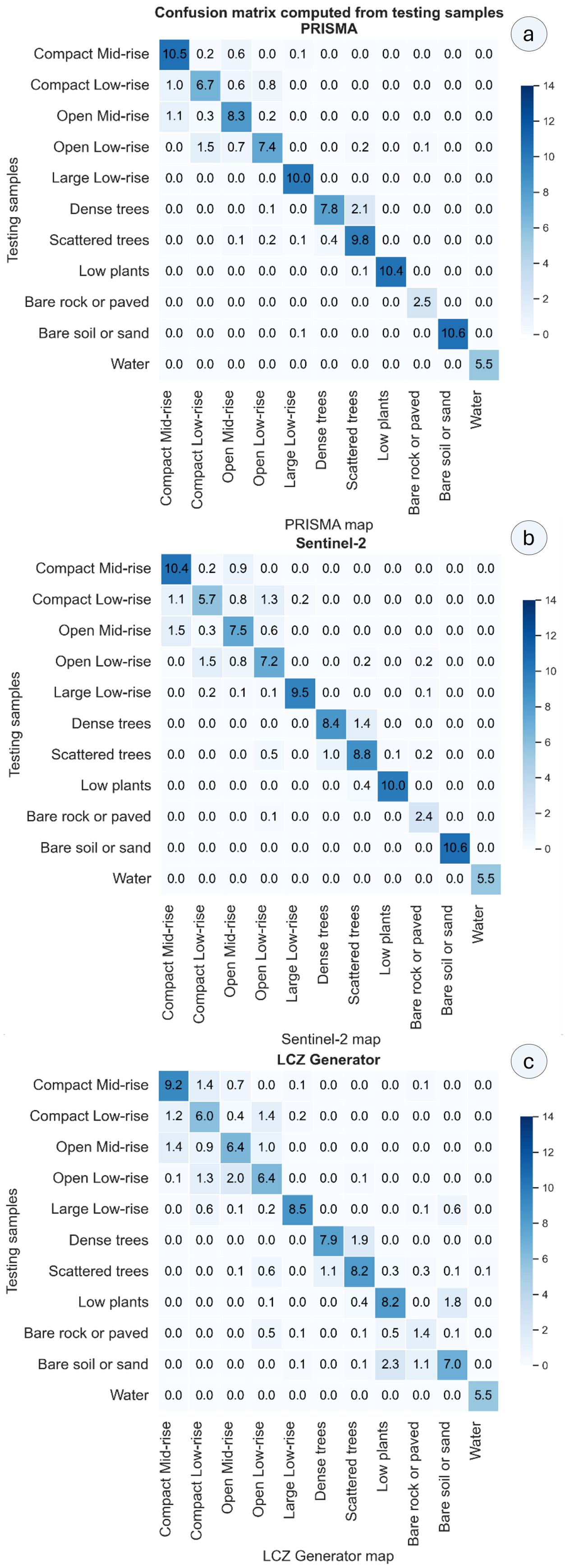

Figure 2. Confusion matrices related to the LCZ maps derived from (a) PRISMA, (b) Sentinel-2 and (c) the LCZ Generator in February 2023.

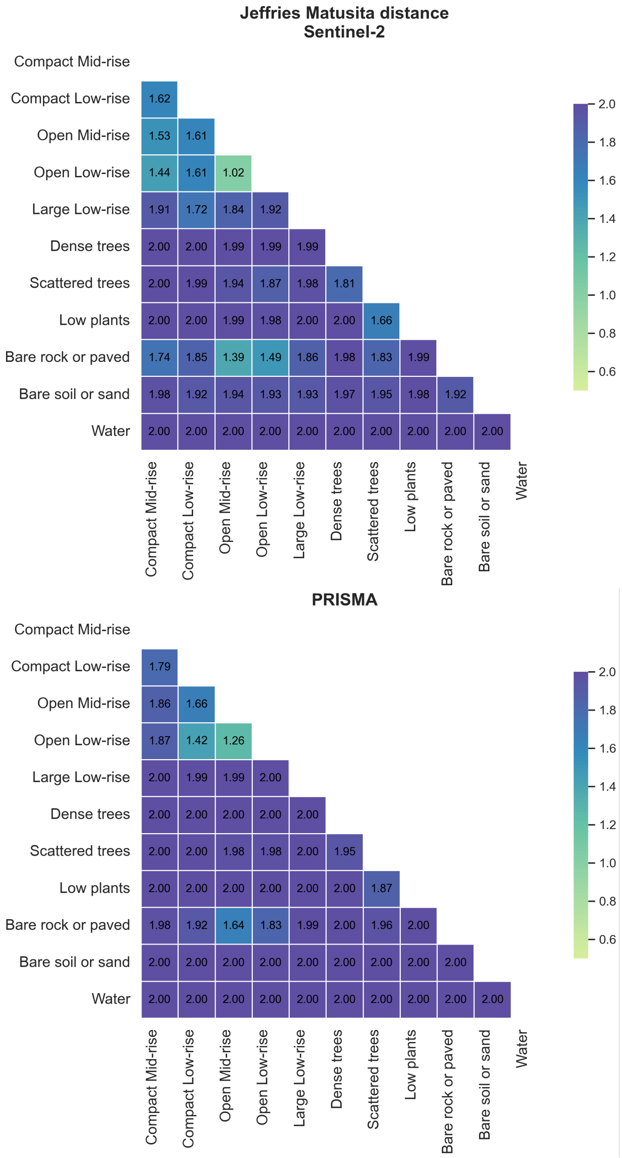

Figure 3. Jeffries-Matusita distance between the spectral signature of training samples, for each couple of LCZ classes computed from Sentinel-2 and PRISMA images acquired in February 2023.

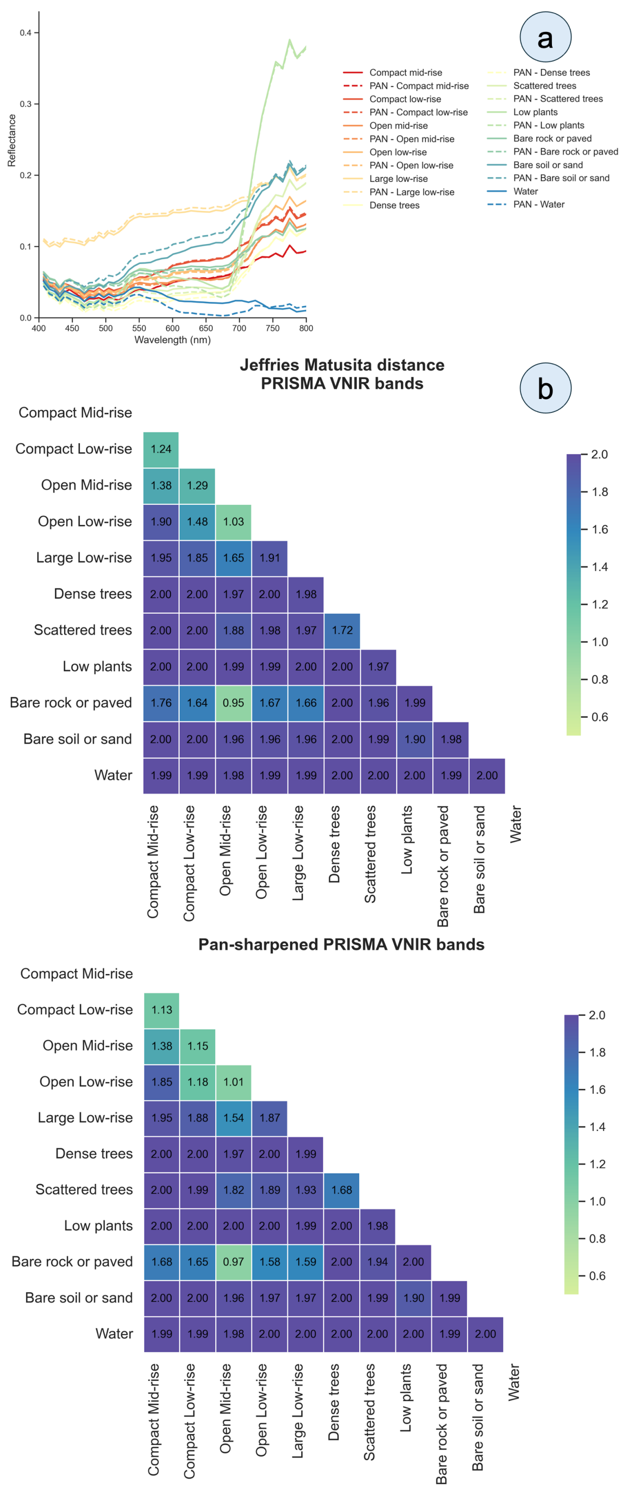

Figure 4. (a) LCZ spectral signatures and (b) Jeffries-Matusita distances between each couple of LCZ classes, computed from the original and pan-sharpened (PAN) PRISMA Visible-NearInfraRed (VNIR) bands, acquired in February 2023.

The qualitative analysis of temperature distribution within different LCZs in the Metropolitan City of Milan confirms the relationship between the urban morphology and land cover characteristics (which define LCZs) and average air temperatures. Disparities in median temperatures with variations of up to 2°C were observed between built-up LCZs compared to vegetated classes, as shown in Figure 5.

4. Conclusions and Outlook

This paper illustrates a comprehensive methodology for LCZ mapping using a hybrid RS and GIS approach. The study focused on leveraging and comparing multispectral Sentinel-2 and hyperspectral PRISMA satellite data for improved LCZ classification in the Metropolitan City of Milan.

The results demonstrate the efficacy of PRISMA data in enhancing LCZ detection accuracy compared to Sentinel-2 and other

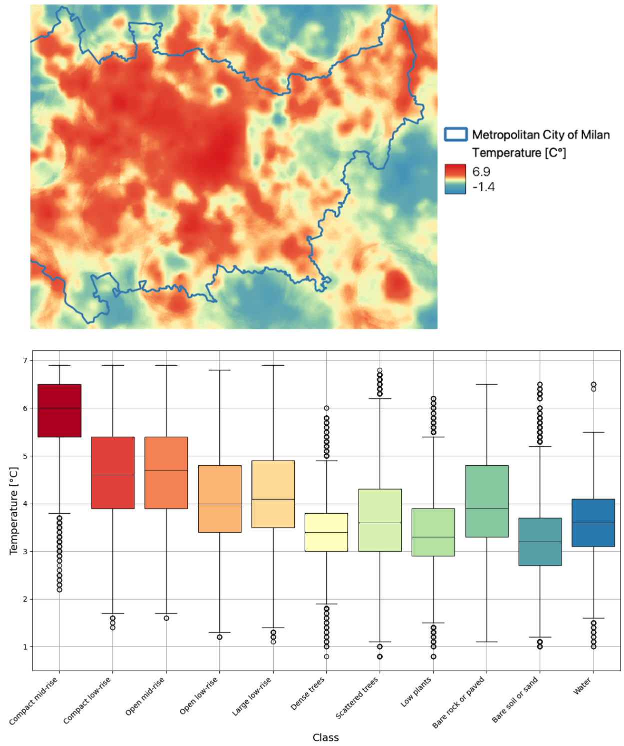

Figure 5. ClimaMi map of average winter nighttime air temperature and boxplots summarizing the temperature distributions in each LCZ class, detected from the PRISMA image acquired in February 2023. The black lines inside the boxes represent the median temperature.

reference LCZ classification methods such as the LCZ Generator. The overall accuracy increase observed across multiple maps suggests the potential of hyperspectral data in refining LCZ classification.

Spectral separability analysis further highlights the advantage of hyperspectral data over multispectral in differentiating LCZ classes, with PRISMA exhibiting greater distances between spectral signatures. This confirms a higher discriminative capability of hyperspectral imagery, which is critical for an accurate classification and mapping of LCZs.

Furthermore, the study explored the impact of hyperspectral pan-sharpening on LCZ classification, revealing promising results in preserving spectral signatures while enhancing spatial resolution. This approach can offer a viable solution for improving the spatial detail of LCZ maps without sacrificing classification accuracy. However, the quantitative assessment of pan-sharpening accuracy is left as a future development of this work.

Finally, the qualitative analysis of temperature distributions within different LCZs underscores the importance of urban morphology and land cover characteristics in influencing local climate conditions. The observed temperature disparities between built-up and vegetated LCZs emphasize the role of urban planning and design in mitigating the HUI effects and promoting urban thermal comfort.

Formal analysis of correlations between LCZs and local air temperature patterns in the Metropolitan City of Milan will be taken into consideration in the future development of this work with the aim of providing actionable insights to urban planners for climate-proof land management.

The methodological workflow used in this study relies entirely on free and open-source technologies to facilitate future revisions and replications of the case study addressed in this paper and beyond. The same applies to the whole results of the LCZ-ODC project.

Acknowledgements

This work was developed within the LCZ-ODC project, funded by the Italian Space Agency (ASI) (agreement n. 2022-30-HH.0) in the framework of the Innovation for Downstream Preparation for Science (I4DP_SCIENCE) program.

References

Aslam, A., Rana, I. A., 2022. The use of local climate zones in the urban environment: A systematic review of data sources, methods, and themes. *Urban Climate*, 42, 101120.

Demuzere, M., Kittner, J., Bechtel, B., 2021. LCZ Generator: a web application to create Local Climate Zone maps. *Frontiers in Environmental Science*, 9, 637455.

Kumar, P., 2021. Climate change and cities: challenges ahead. *Frontiers in Sustainable Cities*, 3, 645613.

Lehnert, M., Geletič, J., Dobrovolnỳ, P., Jurek, M., 2018. Temperature differences among local climate zones established by mobile measurements in two central European cities. *Climate Research*, 75(1), 53–64.

Liang, Y., Song, W., Cao, S., Du, M., 2023. Local Climate Zone Classification using daytime Zhuhai-1 hyperspectral imagery and nighttime light data. *Remote Sensing*, 15(13), 3351.

Loizzo, R., Daraio, M., Guarini, R., Longo, F., Lorusso, R., Dini, L., Lopinto, E., 2019. Prisma mission status and perspective. *IGARSS 2019-2019 IEEE International Geoscience and Remote Sensing Symposium*, IEEE, 4503–4506.

Loncan, L., De Almeida, L. B., Bioucas-Dias, J. M., Briottet, X., Chanussot, J., Dobigeon, N., Fabre, S., Liao, W., Licciardi, G. A., Simoes, M. et al., 2015. Hyperspectral pansharpening: A review. *IEEE Geoscience and remote sensing magazine*, 3(3), 27–46.

Oxoli, D., Cedeno Jimenez, J., Capizzi, E., Brovelli, M., Siciliani de Cumis, M., Sacco, P., Tapete, D., 2023. QGIS and Open Data Cube applications for local climate zones analysis leveraging PRISMA hyperspectral satellite data. *ISPRS-International Archives of the Photogrammetry, Remote Sensing and Spatial Information Sciences*, 48, 111–116.

Richards, J. A., Jia, X., 2006. Interpretation of hyperspectral image data. *Remote sensing digital image analysis: An introduction*, 359–388.

Stewart, I. D., Oke, T. R., 2012. Local climate zones for urban temperature studies. *Bulletin of the American Meteorological Society*, 93(12), 1879–1900.

Stewart, I. D., Oke, T. R., Krayenhoff, E. S., 2014. Evaluation of the 'local climate zone scheme' using temperature observations and model simulations. *International journal of climatology*, 34(4), 1062–1080.

Vavassori, A., Brovelli, M., Capizzi, E., Venuti, G., Betti, B., Siciliani de Cumis, M., Sacco, P., Tapete, D., 2023a. Mapping Local Climate Zones with multiple geodata and the Open Data Cube: Insights of domain user requirements and outlooks of the LCZ-ODC Project. *ISPRS-International Archives of the Photogrammetry, Remote Sensing and Spatial Information Sciences*, 48, 581–587.

Vavassori, A., Giuliani, G., Brovelli, M. A., 2023b. Mapping Local Climate Zones in Lausanne (Switzerland) with Sentinel-2 and PRISMA imagery: comparison of classification performance using different band combinations and building height data. *International Journal of Digital Earth*, 16(2), 4790–4810.